

p-Wave Cold Collisions in an Optical Lattice Clock

N. D. Lemke,^{1,*} J. von Stecher,² J. A. Sherman,¹ A. M. Rey,² C. W. Oates,¹ and A. D. Ludlow^{1,†}

¹National Institute of Standards and Technology, Boulder, CO 80305, USA

²JILA, NIST and University of Colorado, Department of Physics, Boulder, CO 80309, USA

(Dated: November 9, 2021)

We study ultracold collisions in fermionic ytterbium by precisely measuring the energy shifts they impart on the atom's internal clock states. Exploiting Fermi statistics, we uncover *p*-wave collisions, in both weakly and strongly interacting regimes. With the higher density afforded by two-dimensional lattice confinement, we demonstrate that strong interactions can lead to a novel suppression of this collision shift. In addition to reducing the systematic errors of lattice clocks, this work has application to quantum information and quantum simulation with alkaline-earth atoms.

Ultracold alkaline-earth atoms trapped in an optical field are rich physical systems and attractive candidates for quantum information processing [1–4], quantum simulation of many-body Hamiltonians [5–9], and quantum metrology [10–14]. In each case, interrogating many atoms simultaneously facilitates high measurement precision, but can also yield high atomic density and the potential for atom-atom collisions at lattice sites with multiple atoms. For quantum information and simulation, these interactions can be a key feature; for quantum metrology, however, they present an undesired complication. In either case, these interactions need to be well understood.

To limit interactions in lattice clocks, the use of ultracold, spin-polarized fermions was proposed to exploit the Fermi suppression of *s*-wave collisions while freezing out higher partial-wave contributions. However, small collision shifts have been measured in fermionic ⁸⁷Sr [11, 15–19] and ¹⁷¹Yb [12]. Aided by the quantum statistics that govern the interactions of these fermionic atoms, we present a complete picture of the cold collisions in the Yb lattice clock by performing measurements with state-of-the-art precision together with a quantitative theoretical model. While with Sr it was found that *s*-wave collisions can occur in the presence of excitation inhomogeneity, with Yb we highlight here the important role that *p*-wave collisions can play in lattice clock systems. Moreover, we demonstrate techniques for canceling the collision shift that could be used to vastly reduce the clock uncertainty.

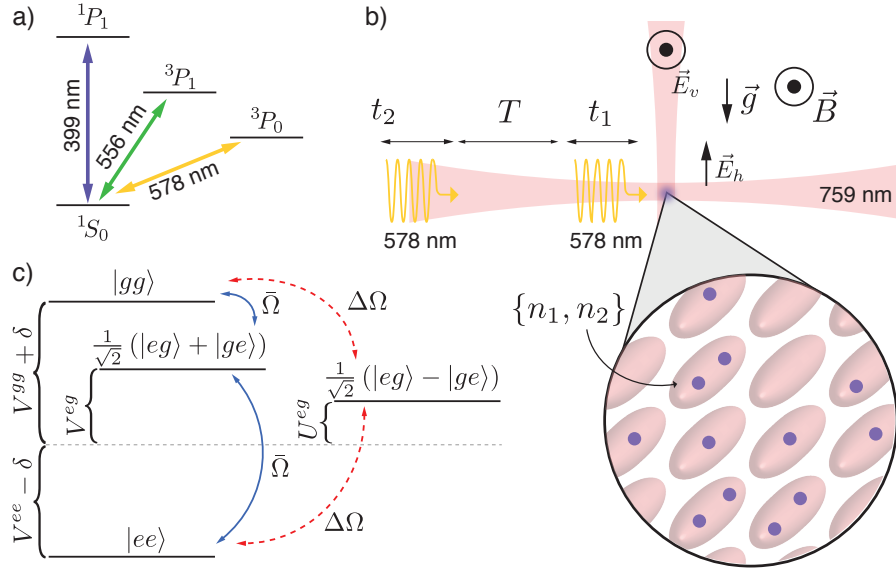


FIG. 1: (a) Energy level diagram for Yb. (b) Schematic of the two lattices. Arrows indicate optical polarizations and magnetic field directions with respect to gravity. At the left, the Ramsey pulse sequence is entering: two pulses of times $t_{1,2}$ separated by dark time T (not to scale). An inset shows a few 2-D lattice sites with 0 to 2 atoms per site; two atoms in one of the sites occupy axial motional states n_1 and n_2 . (c) Energy level diagram for two atoms in the rotating frame: three triplet states and one singlet state, with interactions V and U , as in Eq. (1).

To determine the nature of the collisions, here we use two-pulse Ramsey spectroscopy [20] (Fig. 1). Provided the Ramsey pulse times $t_{1,2}$ are short compared to the dark time T , the vast majority of the collisions occur while the population is not being simultaneously driven by the laser field, simplifying the analysis of the interactions.

The Ramsey technique also eliminates a strong laser-detuning-dependence on the excitation evolution and thus the interaction dynamics. Finally, the Ramsey scheme offers the possibility to explore proposals for cancelation of the cold collision shift by tailoring the Ramsey pulses [16].

In addition to measurements of the collision shift with atoms confined in a one-dimensional (1-D) optical lattice, we also show results from a two-dimensional (2-D) lattice, which offers several benefits. First, with strong confinement in all but one dimension, the collisions can be treated with a 1-D model. Second, the higher number of lattice sites in a 2-D lattice reduces the lattice's overfilling (i.e., many atoms per site). Finally, the 2-D lattice offers stronger interactions at any lattice sites that are doubly occupied.

To model the collisions in a 2-D lattice, we begin by considering a simple case: two atoms in the same lattice site, populating axial vibrational modes n_1 and n_2 and the lowest transverse band [4, 5, 17]. Assuming the vibrational quantum numbers are conserved during the collisions and laser interrogation, the Hamiltonian for the two-atom system can be written in a four-state basis set: $|gg\rangle$, $|ee\rangle$, $(|eg\rangle + |ge\rangle)/\sqrt{2}$ (“triplet states”) and $(|eg\rangle - |ge\rangle)/\sqrt{2}$ (“singlet state”) [16, 19]. Here g and e are associated with the lowest 1S_0 and 3P_0 electronic levels, respectively, which are coupled by the probe laser. The Hamiltonian in the rotating frame can be written in this basis as

$$H_T = \begin{pmatrix} \delta + V_{n_1, n_2}^{gg} & 0 & \frac{\bar{\Omega}_{n_1, n_2}}{\sqrt{2}} & \frac{\Delta\Omega_{n_1, n_2}}{\sqrt{2}} \\ 0 & -\delta + V_{n_1, n_2}^{ee} & \frac{\bar{\Omega}_{n_1, n_2}}{\sqrt{2}} & -\frac{\Delta\Omega_{n_1, n_2}}{\sqrt{2}} \\ \frac{\bar{\Omega}_{n_1, n_2}}{\sqrt{2}} & \frac{\bar{\Omega}_{n_1, n_2}}{\sqrt{2}} & V_{n_1, n_2}^{eg} & 0 \\ \frac{\Delta\Omega_{n_1, n_2}}{\sqrt{2}} & -\frac{\Delta\Omega_{n_1, n_2}}{\sqrt{2}} & 0 & U_{n_1, n_2}^{eg} \end{pmatrix}. \quad (1)$$

Here δ is the detuning from the atomic transition, $\bar{\Omega}_{n_1, n_2} = (\Omega_{n_1} + \Omega_{n_2})/2$ is the average Rabi frequency for the two atoms, and $\Delta\Omega = (\Omega_{n_1} - \Omega_{n_2})/2$ is the difference in Rabi frequency. The dependence of the Rabi frequency on the axial vibrational state is caused by any small projection of the probe beam along the axial direction. The terms U_{n_1, n_2}^{eg} and $V_{n_1, n_2}^{\alpha\beta}$ give, respectively, the s - and p -wave interactions between an $\alpha = g, e$ and a $\beta = g, e$ atom [21]. Because the atomic population is prepared in a single nuclear-spin state ($m_I = 1/2$ or $-1/2$), quantum statistics dictates that only the triplet states, which are invariant under particle exchange, are affected by p -wave interactions, while the singlet configuration interacts via s -wave only.

For short pulses and large Rabi frequencies, we can ignore interaction effects during the pulses. During the Ramsey dark time, the Hamiltonian describing the atom dynamics is diagonal in the singlet-triplet basis, and each state acquires just a phase. Consequently, after the second pulse is applied, we recover Ramsey fringes with a frequency shift. To compare with the 2-D lattice experiment, the shift must be integrated over the atomic distribution within an array of singly and doubly occupied lattice sites. Moreover, instead of choosing a specific set of vibrational modes $\{n_1, n_2\}$, we numerically calculate the appropriate thermal average over all possible modes [21]. In the 1-D lattice, each site is populated by many atoms, so the two-atom model is not directly applicable. However, in the weakly interacting regime, a mean-field picture that approximates the many-atom interactions by a sum of pairwise interactions provides a fair description, so we use the two-atom Hamiltonian with temperature-dependent, effective interaction parameters to model the multi-atom case. We compared this effective model with a numerically calculated N-body model and found qualitative agreement.

Our experimental procedures are similar to those described in [12]. After two stages of laser cooling (see Fig. 1(a)), atoms are trapped by the horizontal or vertical lattice for 1-D confinement, or by both lattices for 2-D operation. In the latter case, we filter away any atoms that are not fully confined at the intersection of the beams by adiabatically decreasing the power in one dimension to zero before turning it back up, then doing the same for the other lattice. Approximately 2.5×10^4 atoms are trapped in the 1-D lattice, while $\frac{1}{5}$ as many remain in the 2-D lattice after filtering. In the 1-D lattice this corresponds to an estimated density of $\rho_1 = 3 \times 10^{11}/\text{cm}^3$ and ~ 20 atoms per site; for the 2-D lattice, we estimate that 25 % of the atoms are in doubly-occupied sites, for which the effective density is $\rho_2 = 4 \times 10^{12}/\text{cm}^3$, and fewer than 1 % of the atoms are in sites with more than two atoms. The trap frequencies in the lattice were typically 50-75 kHz in the strong direction(s) and 300-500 Hz in the weak direction(s). The lattice is tuned to the “magic wavelength” near 759 nm, where the two clock states experience identical trapping potentials. We offset the frequencies of the two lattice beams by 2 MHz using acousto-optic modulators (AOMs), preventing any line-broadening from the vector Stark shift [12, 22–24].

With the atoms loaded in a lattice, we spin-polarize the sample by optical pumping to one of the spin states ($m_F = \pm 1/2$) with 556 nm light; impurity in the spin-polarization is below 1 %. The clock light, pre-stabilized to a high-finesse optical cavity [25] to be resonant with the $^1S_0 \rightarrow ^3P_0$ clock transition, is switched on during the Ramsey pulses with an AOM. We interleave high- and low-density clock conditions, each with its own set of integrators to lock

the clock laser to the atomic transition and to average over both $m_F = \pm 1/2$ spin states. The collisional frequency shift is found by looking at the difference of the correction signals applied to the AOM divided by the difference in atom number, which is typically varied by changing the power to the 399 nm slowing beam that opposes the atomic beam. These interleaved measurements have an instability of $\leq 1.5 \times 10^{-15}/\sqrt{\tau}$, for averaging time τ in seconds, allowing statistical error bars of ~ 20 mHz in just 2000 s.

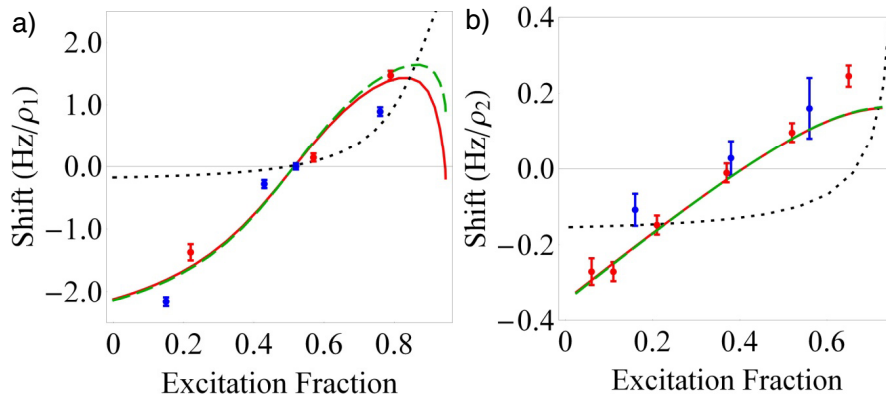


FIG. 2: (a) Collision shift vs excitation fraction, 1-D lattice. Blue (red) points show experimental measurements in a vertical (horizontal) lattice with temperature $\mathcal{T} \sim 10 \mu\text{K}$ and $\langle \Delta\Omega/\Omega \rangle_{\mathcal{T}} = 0.2$. Dashed black line gives an s -wave-only fit ($\langle U^{eg} \rangle_{\mathcal{T}} = -2\pi \times 1.5$ Hz) from the mean-field model. Solid red line gives a p -wave-only fit with $\langle V^{eg} \rangle_{\mathcal{T}} = 10 \langle V^{ee} \rangle_{\mathcal{T}} = -2\pi \times 1.1$ Hz. Long-dashed green line adds to this a small s -wave component ($\langle U^{eg} \rangle_{\mathcal{T}} = -2\pi \times 0.6$). (b) Collision shift vs excitation fraction, 2-D lattice. Blue (red) points probe along the vertical (horizontal) lattice. Dashed black line is an s -wave-only fit with $a_{eg}^- \approx -25 a_0$ (a_0 the Bohr radius); solid red line is a p -wave-only fit with $b_{eg} \approx -74 a_0$ and $b_{ee}^3 = 0.1b_{eg}^3$. The long-dashed green line adds to this a small s -wave interaction $a_{eg}^- = -25 a_0$.

We first considered the collisional shift as a function of excitation fraction (i.e., the fraction in $|e\rangle$ during the Ramsey dark time). The excitation fraction was varied by changing the Rabi frequency of the Ramsey pulses. The measured shift for atoms in a 1-D lattice is shown in Fig. 2(a) (blue and red points), and for atoms in a 2-D lattice in Fig. 2(b). For these data, the Ramsey pulse time is $t_1 = t_2 = 1$ ms, and the dark time is $T = 80$ ms. For the 2-D lattice the black dashed and solid red curves give the numerically calculated shift using the s -wave scattering length (a_{eg}^-) and p -wave scattering volumes (b_{eg}^3 and b_{ee}^3) as fitting parameters. (V^{gg} is taken to be zero, consistent with prior measurements [26]). For the 1-D lattice, the curves are calculated from the mean-field approximation with the effective interaction parameters, which are required to be consistent with those used for the 2-D lattice calculations, varied for fitting.

Because the atoms are prepared in the triplet state $|gg\rangle$, s -wave interactions are allowed only in the presence of inhomogeneity ($\Delta\Omega_{n_1, n_2} \neq 0$), which transfers population to the singlet state. The collisions observed in ^{87}Sr have been attributed to this type of interaction [15–19]. By contrast, p -wave interactions are fully allowed, provided there is sufficient collision energy to overcome the centrifugal barrier (expected to exceed $30 \mu\text{K}$ based on calculated van der Waals coefficients [27]). As shown in the figure, the p -wave interaction provides a much better description of the experimental data, as the shift induced by pure s -wave collisions is generally too small and does not exhibit the correct dependence on the excitation fraction. The shifts go through zero near an excitation fraction of 0.51 in the 1-D lattice and 0.4 in the 2-D lattice. Zero-crossings near 0.5 are readily understood if V^{eg} dominates: by creating equal partial densities of ground and excited atoms, the energy shift on the two clock levels is the same, and the net shift is canceled. This effect could allow for vast reduction to the collisional shift in the Yb lattice clock. The deviation from a zero-crossing at exactly 0.5 in the 1-D case is consistent with a small ee interaction ($b_{ee}^3 = 0.1b_{eg}^3$, with $b_{eg} \approx -74 a_0$ and a_0 the Bohr radius).

We investigated tunneling effects by measuring the shifts for both vertically and horizontally oriented 1-D lattices, exploiting gravity-induced suppression of the tunneling rate [28], but we observed no change in the data (Fig. 2(a)). We estimate the tunneling rate, thermally averaged over the lowest nine bands of the 1-D horizontal lattice, to be several hertz. In the vertical 1-D lattice and the 2-D lattice, this rate is suppressed by more than a factor of ten due to the energy offset between adjacent sites (arising from gravity [28] and the Gaussian beam profile). However, the two highest bands of the lattice, which are populated with a few percent of the atoms, can have very high tunneling rates (several kilohertz) that are not suppressed by the energy offset. Because of this, the fraction of atoms that can tunnel during the spectroscopic time are 10 %, 5 %, and 10 % for the horizontal, vertical, and 2-D lattices, respectively. We do not see any appreciable difference between the shifts measured in the horizontal and vertical lattices and thus

conclude that tunneling does not play a significant role in the collision shifts.

We use short Ramsey pulses ($t_{1,2} \sim 1$ ms) to avoid interaction effects during the pulse. But, for pulses shorter than the mean oscillation period in the trap, $\Omega \gtrsim \omega_i$, with i the weakest trap direction, and laser-induced mode-changing collisions are not necessarily suppressed. Nevertheless, we ruled out the relevance of those processes by varying the pulse duration over a factor of ten without observing any substantial modification to the measured collision shifts [21]. We looked for dependence of the collision shifts on the second pulse area [16], but found no significant dependencies.

To further rule out s -wave interactions, we misaligned the probe beam to couple more strongly to the weak confinement axis of the lattice trap (Fig. 3(a)). Doing so introduces greater excitation inhomogeneity from the Ramsey pulse (in this case, up to a factor of 2.4) because the atoms are not tightly confined along this axis [15]. We expect the s -wave shift to depend quadratically on the inhomogeneity, yet the frequency shifts show no such dependence. This insensitivity is well explained by p -wave interactions, which depend only weakly on inhomogeneity at these levels (decreasing slightly as more population transfers to the singlet state). A small but non-zero s -wave interaction could balance this effect and may help explain the complete lack of dependence, as shown in the theory curves in Fig. 3(a). The green long-dashed lines in Fig. 2(a,b) also show that adding a small but non-zero s -wave interaction is consistent with the observed collision shifts. Still, all of these considerations indicate that p -wave interactions play the dominant role in the cold collisions of ^{171}Yb .

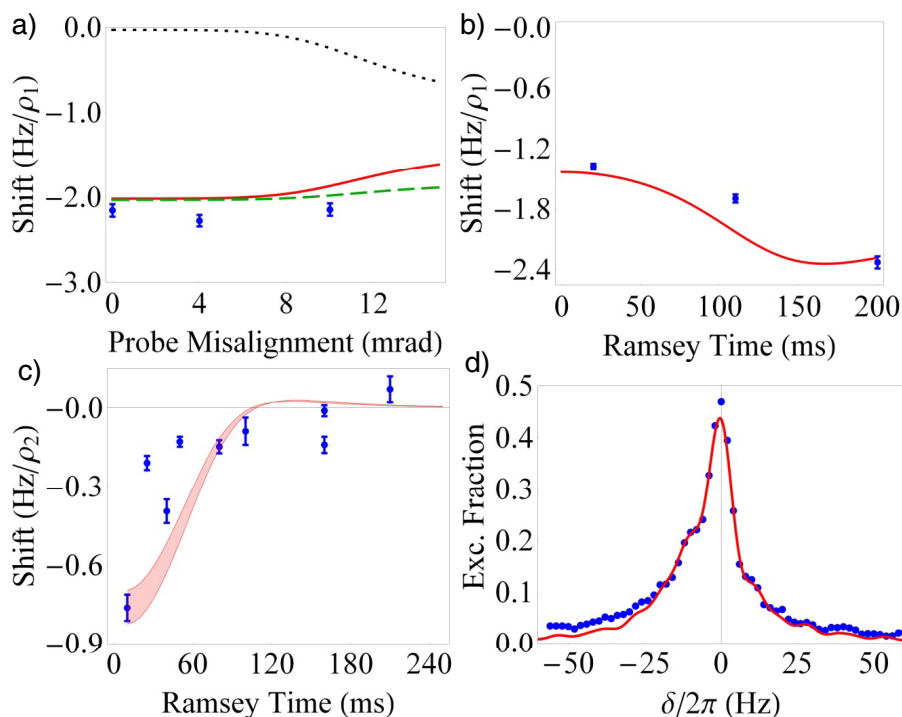


FIG. 3: (a) Collision shift vs probe misalignment angle (vertical 1-D lattice) for constant excitation fraction 0.12. Using the same parameters as Fig. 2(a), the dashed black line gives an s -wave-only fit, solid red line gives a p -wave-only fit, and the long-dashed green line has s - and p -wave terms. In the well-aligned case (0 mrad) there is a residual effective misalignment of ~ 5 mrad due to the imperfect overlap between lattice and probe beams. (b) Collision shift vs Ramsey time, 1-D lattice, for excitation fraction 0.18. Using the same parameters as Fig. 2(a), the solid-line gives a fit from the mean-field model. (c) Collision shift vs Ramsey time, 2-D lattice, for excitation fraction $0.19 \pm .03$. The shift crosses zero due to the periodic dependence of the shift on collisional phase, and is a signature of strong interactions. The model calculations (shaded region) use the same parameters as Fig. 2(b) for an excitation fraction range $0.19 \pm .03$. (d) Asymmetric Rabi spectrum, 2-D lattice. The solid line is the prediction of the model, using the number of doubly occupied sites as a fitting parameter.

Strong interactions emerge in the regime $V^{\alpha\beta}T \geq 1$. A key observation revealing the operation of the 2-D lattice clock in the regime $V^{ge}T \gg V^{ee}T \geq 1$ is the zero-crossing of the collision shift at a lower excitation fraction of 0.4, which deviates from the crossing at 0.5 predicted by the weakly interacting expression of the shift [21]. The interaction strength also introduces additional dependencies on the Ramsey dark time. With weak interactions, the collision shift is independent of T , but with strong interactions the clock shift decays with increasing T due to the shift's sinusoidal dependence on scattering phase [21, 29]. We investigated this experimentally by varying the dark time T and measuring collision shifts in the 1-D lattice (Fig. 3(b)), where the shift scales weakly with T , and the

2-D lattice (Fig. 3(c)), where the shift is strongly damped towards zero with increasing T . Yet a third signature of strong interactions is significant asymmetry in the clock transition spectrum. In Fig. 3(d) we show a Rabi spectrum ($t = 120$ ms), taken under high density operation in the 2-D lattice, which shows an additional feature on the red side ($\delta < 0$) of resonance. This asymmetry is density-dependent and barely observable in the 1-D lattice. In the 2-D lattice, the interactions are sufficiently strong ($V^{egt} \geq 1$) to introduce these asymmetric lineshape features beyond the transition linewidth. With yet higher density, it may be possible to spectrally resolve three features, one each for the s -wave-interacting singlet, the p -wave-interacting triplets, and the non-interacting atoms in singly occupied lattice sites. Interaction-induced sidebands were recently reported in [30] and may be useful for quantum simulation applications.

In this Letter we have shown evidence for p -wave interactions in ultracold Yb confined in an optical lattice. Although lower atomic temperature yields reduced tunneling through the p -wave barrier, and thus a lower scattering cross-section, it also increases the atomic density of the confined atoms. For this reason, both s - and p -wave interactions may be potentially relevant for all optical lattice clock systems. Using the dependence of the measured shift on excitation fraction and Ramsey dark time, we have observed zero-crossings in the measured frequency shifts, which provide the metrological means to reduce the shifts to nearly negligible levels.

The authors gratefully acknowledge assistance from Y. Jiang, S. Diddams, T. Fortier, and M. Kirchner and financial support from NIST, NSF-PFC, AFOSR, ARO, and DARPA-OLE.

* also at Department of Physics, University of Colorado, Boulder, CO 80309, USA

† Electronic address: Electronic address: ludlow@boulder.nist.gov

- [1] D. Hayes, P. S. Julienne, and I. H. Deutsch, Phys. Rev. Lett. **98**, 070501 (2007).
- [2] I. Reichenbach and I. H. Deutsch, Phys. Rev. Lett. **99**, 123001 (2007).
- [3] A. J. Daley, M. M. Boyd, J. Ye, and P. Zoller, Phys. Rev. Lett. **101**, 170504 (2008).
- [4] A. V. Gorshkov, et al., Phys. Rev. Lett. **102**, 110503 (2009).
- [5] A. V. Gorshkov, et al., Nat. Phys. **6**, 289 (2010).
- [6] M. A. Cazalilla, A. F. Ho, and M. Ueda, New Journal of Physics **11**, 103033 (2009).
- [7] M. Foss-Feig, M. Hermele, and A. M. Rey, Phys. Rev. A **81**, 051603 (2010).
- [8] M. Foss-Feig, M. Hermele, V. Gurarie, and A. M. Rey, Phys. Rev. A **82**, 053624 (2010).
- [9] M. Hermele, V. Gurarie, and A. M. Rey, Phys. Rev. Lett. **103**, 135301 (2009).
- [10] H. Katori, M. Takamoto, V. G. Pal'chikov, and V. D. Ovsiannikov, Phys. Rev. Lett. **91**, 173005 (2003).
- [11] A. D. Ludlow, et al., Science **319**, 1805 (2008).
- [12] N. D. Lemke, et al., Phys. Rev. Lett. **103**, 063001 (2009).
- [13] R. Le Targat, et al., Phys. Rev. Lett. **97**, 130801 (2006).
- [14] T. Akatsuka, M. Takamoto, and H. Katori, Nat. Phys. **4**, 954 (2008).
- [15] G. K. Campbell, et al., Science **324**, 360 (2009).
- [16] K. Gibble, Phys. Rev. Lett. **103**, 113202 (2009).
- [17] A. M. Rey, A. V. Gorshkov, and C. Rubbo, Phys. Rev. Lett. **103**, 260402 (2009).
- [18] Z. Yu and C. J. Pethick, Phys. Rev. Lett. **104**, 010801 (2010).
- [19] M. D. Swallows, et al., Science **331**, 1043 (2011).
- [20] N. F. Ramsey, Phys. Rev. **78**, 695 (1950).
- [21] See Supplementary Material for further details of the theoretical model and experimental parameters.
- [22] S. G. Porsev, A. Derevianko, and E. N. Fortson, Phys. Rev. A **69**, 021403 (2004).
- [23] C. Chin, et al., Phys. Rev. A **63**, 033401 (2001).
- [24] J. Sebby-Strabley, M. Anderlini, P. S. Jessen, and J. V. Porto, Phys. Rev. A **73**, 033605 (2006).
- [25] Y. Y. Jiang, et al., Nat. Photon. **5**, 158 (2011).
- [26] M. Kitagawa, et al., Phys. Rev. A **77**, 012719 (2008).
- [27] V. A. Dzuba and A. Derevianko, J. Phys. B **43**, 074011 (2010).
- [28] P. Lemonde and P. Wolf, Phys. Rev. A **72**, 033409 (2005).
- [29] K. Gibble, 2010 IEEE International Frequency Control Symposium (Fcs) pp. 56–58 (2010).
- [30] M. Bishof, et al., arXiv:1102.1016v2 (2011).

Supplementary Material

TWO ATOM MODEL

Here we consider two nuclear-spin-polarized fermionic atoms interacting via s -wave and p -wave channels. The atoms are confined in a tube with frozen transverse degrees of freedom (only the lowest vibrational transverse mode is populated). Along the tube direction, \hat{Z} , there is a weak harmonic confinement with frequency ω_Z , and we will first assume the two atoms populate the vibrational modes n_1 and n_2 . In this case there are only four states spanning the Hilbert space: the triplet states $|gg\rangle$, $|ee\rangle$, $(|eg\rangle + |ge\rangle)/\sqrt{2}$, and the singlet, $(|eg\rangle - |ge\rangle)/\sqrt{2}$. Here the convention used is that the left atom populates mode n_1 and the right atom mode n_2 .

In the presence of a laser field with wave vector $\mathbf{k} = k_Y \hat{Y} + k_Z \hat{Z}$ and detuned from the atom transition frequency by δ , the two-atom Hamiltonian in the rotating frame reduces to Eq. 1 in the main text. Here $\Omega_n = \Omega_0 L_n(\eta_Z^2) L_0(\eta_Y^2) e^{-(\eta_Y^2 + \eta_Z^2)/2}$, with $\eta_i = k_i \sqrt{\frac{\hbar}{2m\omega_i}}$ the Lamb-Dicke parameter along the i direction, Ω_0 the bare Rabi frequency, and L_n the Laguerre polynomial. m is the atom mass. The s -wave and p -wave interaction parameters are $U_{n_j, n_{j'}}^{eg} \equiv 4 \frac{\sqrt{m\omega_X \omega_Y \omega_Z}}{\sqrt{\hbar}} a_{eg}^- S_{n_j, n_{j'}}$ and $V_{n_j, n_{j'}}^{\alpha\beta} \equiv 12 \frac{\sqrt{m^3 \omega_X \omega_Y \omega_Z^3}}{\sqrt{\hbar^3}} b_{\alpha, \beta}^3 P_{n_j, n_{j'}}$. Here $S_{n_j, n_{j'}}$ and $P_{n_j, n_{j'}}$ are geometric terms that take into account the spatial overlap between the atomic wavefunctions of colliding atoms in modes n_j and $n_{j'}$. They are given by $S_{nn'} = \frac{\int d\xi e^{-2\xi^2} H_n^2(\xi) H_{n'}^2(\xi) d\xi}{\sqrt{4^{n+n'} n!^2 n'!^2}}$ and $P_{nn'} = \frac{\int d\xi e^{-2\xi^2} \left(\frac{dH_n(\xi)}{d\xi} H_{n'}(\xi) - H_n(\xi) \frac{dH_{n'}(\xi)}{d\xi} \right)^2}{\sqrt{4^{n+n'} n!^2 n'!^2}}$, where H_n are Hermite polynomials. The dependence of $V^{\alpha\beta}$ and U^{eg} on the vibrational mode encapsulates the temperature dependence of the interactions.

We ignore interactions during the pulses, and consequently the number of excited atoms after the first pulse is

$$N_{n_1, n_2}^e(t_1) = 1 - \cos(\bar{\Omega}_{n_1, n_2} t_1) \cos(\Delta\Omega_{n_1, n_2} t_1), \quad (2)$$

During the dark time, the Hamiltonian is diagonal and each state acquires just a phase. After the second pulse, the excited state population is

$$N_{n_1, n_2}^e(t_1, t_2) = A_{n_1, n_2} + \mathcal{N}_{n_1, n_2} \cos[(\delta - 2\pi\Delta\nu_{n_1, n_2}^{ge})T], \quad (3)$$

with A_{n_1, n_2} an overall offset, $\mathcal{N}_{n_1, n_2} > 0$ the fringe amplitude, and $\Delta\nu_{n_1, n_2}^{ge}$ the frequency shift. These quantities can be computed analytically.

In the 2-D lattice system an array of isolated tubes is populated with mainly one and two atoms per tube. If N_0 tubes are singly occupied and N_1 tubes doubly occupied, then

$$N_{n_1, n_2}^e(t_1, t_2) = \tilde{A}_{n_1, n_2}^e + \cos[\delta T] (\mathcal{A}_{n_1, n_2}^1 + \mathcal{A}_{n_1, n_2}^{2e}) + \sin[\delta T] \mathcal{B}_{n_1, n_2}^e, \quad (4)$$

with

$$\tilde{A}_{n_1, n_2}^e = \sum_{i=1}^{N_1} [1 - \sin(\Delta\theta_1^i) \sin(\Delta\theta_2^i) \sin(\theta_1^i) \sin(\theta_2^i) \cos(2T(V_i^{e\mathcal{E}} - U_i^{e\mathcal{E}})) - \cos(\Delta\theta_1^i) \cos(\Delta\theta_2^i) \cos(\theta_1^i) \cos(\theta_2^i)] \quad (5)$$

$$+ \frac{1}{2} \sum_{i=1}^{N_0} [1 - \sin(\Delta\theta_1^i) \sin(\Delta\theta_2^i) \sin(\theta_1^i) \sin(\theta_2^i) - \cos(\Delta\theta_1^i) \cos(\Delta\theta_2^i) \cos(\theta_1^i) \cos(\theta_2^i)];$$

$$\mathcal{B}_{n_1, n_2}^e = \frac{1}{2} \sum_{i=1}^{N_1} \quad (6)$$

$$- \cos(TC_i) [\cos(\Delta\theta_2^i) \sin(2\theta_1^i) \sin(\theta_2^i) \sin(TB_i) + \sin(2\Delta\theta_1^i) \sin(\Delta\theta_2^i) \cos(\theta_2^i) \sin(TD_i)]$$

$$+ 2 \sin(\Delta\theta_1^i) \sin(\Delta\theta_2^i) \cos(\theta_1^i) \cos(\theta_2^i) \sin(TC_i) \cos(TD_i) + \cos(\Delta\theta_1^i) \cos(\Delta\theta_2^i) \sin(\theta_1^i) \sin(\theta_2^i) [\sin(T(V_i^{ee} - V_i^{e\mathcal{E}})) + \sin(T(V_i^{e\mathcal{E}} - V_i^{g\mathcal{E}}))];$$

$$\mathcal{A}_{n_1, n_2}^1 = \frac{1}{2} \sum_{i=1}^{N_0} (\cos\theta_1^i \cos\theta_2^i \sin\Delta\theta_2^i \sin\Delta\theta_1^i + \cos\Delta\theta_1^i \cos\Delta\theta_2^i \sin\theta_2^i \sin\theta_1^i) \quad (7)$$

$$\mathcal{A}_{n_1, n_2}^{2e} = \frac{1}{2} \sum_{i=1}^{N_1} \quad (8)$$

$$\cos(\Delta\theta_2^i) \sin(\theta_1^i) \sin(\theta_2^i) [2 \cos(\theta_1^i) \sin(TB_i) \sin(TC_i) + \cos(\Delta\theta_1^i) (\cos(T(V_i^{ee} - V_i^{e\mathcal{E}})) + \cos(T(V_i^{e\mathcal{E}} - V_i^{g\mathcal{E}})))] +$$

$$\sin(\Delta\theta_2^i) \cos(\theta_2^i) [\sin(2\Delta\theta_1^i) \sin(TC_i) \sin(TD_i) + \sin(\Delta\theta_1^i) \cos(\theta_1^i) (\cos(T(U_i^{e\mathcal{E}} - V_i^{ee})) + \cos(T(U_i^{e\mathcal{E}} - V_i^{g\mathcal{E}})))]].$$

In the above equations, the dependence of the various parameters on the modes $\{n_1, n_2\}$ is omitted for simplicity but implied. The index i runs over the set of doubly- and singly-occupied tubes. $(V_i^{ee} - V_i^{g\mathcal{E}}) = 2C_i$, $(V_i^{ee} - 2V_i^{e\mathcal{E}} + V_i^{g\mathcal{E}}) =$

$2B_i$, and $(-2U_i^{eg} + V_i^{ee} + V_i^{gg}) = 2D_i$. Due to the Gaussian profile of the laser beams, the trapping confinement varies from tube to tube. This variation gives rise to tube-dependent interaction parameters as well as tube-dependent Rabi frequencies $\theta_s^i = t_s \bar{\Omega}^i$ and $\Delta\theta_s^i = t_s \Delta\Omega^i$. Here $s = 1, 2$.

If the atomic population is initially prepared in the excited state ($|e\rangle$) instead of the ground state ($|g\rangle$), then

$$N_{n_1, n_2}^g(t_1, t_2) = \tilde{A}_{n_1, n_2}^g + \cos[\delta T] (\mathcal{A}_{n_1, n_2}^1 + \mathcal{A}_{n_1, n_2}^{2g}) + \sin[\delta T] \mathcal{B}_{n_1, n_2}^g, \quad (9)$$

with

$$\tilde{A}_{n_1, n_2}^g = \sum_{i=1}^{N_1} [1 + \sin(\Delta\theta_1^i) \sin(\Delta\theta_2^i) \sin(\theta_1^i) \sin(\theta_2^i) \cos(2T(V_i^{eg} - U_i^{eg})) + \cos(\Delta\theta_1^i) \cos(\Delta\theta_2^i) \cos(\theta_1^i) \cos(\theta_2^i)] \quad (10)$$

$$+ \frac{1}{2} \sum_{i=1}^{N_0} [1 + \sin(\Delta\theta_1^i) \sin(\Delta\theta_2^i) \sin(\theta_1^i) \sin(\theta_2^i) + \cos(\Delta\theta_1^i) \cos(\Delta\theta_2^i) \cos(\theta_1^i) \cos(\theta_2^i)];$$

$$\mathcal{B}_{n_1, n_2}^g = \frac{1}{2} \sum_{i=1}^{N_1} \quad (11)$$

$$\cos(\Delta\theta_2^i) \sin(\theta_2^i) [\sin(2\theta_1^i) \sin(TB_i) \cos(TC_i) + \cos(\Delta\theta_1^i) \sin(\theta_1^i) (\sin(T(V_i^{ee} - V_i^{eg})) + \sin(T(V_i^{eg} - V_i^{gg})))] +$$

$$\sin(\Delta\theta_2^i) \cos(\theta_2^i) [2 \sin(\Delta\theta_1^i) \cos(\theta_1^i) \sin(TC_i) \cos(TD_i) + \sin(2\Delta\theta_1^i) \cos(TC_i) \sin(TD_i)];$$

$$\mathcal{A}_{n_1, n_2}^{2g} = \frac{1}{2} \sum_{i=1}^{N_1} \quad (12)$$

$$\cos(\Delta\theta_2^i) \sin(\theta_1^i) \sin(\theta_2^i) [\cos(\Delta\theta_1^i) (\cos(T(V_i^{ee} - V_i^{eg})) + \cos(T(V_i^{eg} - V_i^{gg}))) - 2 \cos(\theta_1^i) \sin(TB_i) \sin(TC_i)]$$

$$+ \sin(\Delta\theta_2^i) \cos(\theta_2^i) [\sin(\Delta\theta_1^i) \cos(\theta_1^i) (\cos(T(U_i^{eg} - V_i^{ee})) + \cos(T(U_i^{eg} - V_i^{gg}))) - \sin(2\Delta\theta_1^i) \sin(TC_i) \sin(TD_i)].$$

In both cases the shift is given by

$$\langle \Delta\nu \rangle_{\mathcal{T}} = \frac{\arctan\left(\frac{\langle \mathcal{B}_{n_1, n_2} \rangle_{\mathcal{T}}}{\langle \mathcal{A}_{n_1, n_2}^2 + \mathcal{A}_{n_1, n_2}^1 \rangle_{\mathcal{T}}}\right) + \pi p}{2\pi T}, \quad (13)$$

with $\langle \rangle_{\mathcal{T}}$ denoting a thermal average. p is an integer that needs to be chosen so that during the $g \rightarrow e$ ($e \rightarrow g$) interrogation the total number of atoms driven to e (g) reaches a maximum value at $\delta = 2\pi \langle \Delta\nu \rangle_{\mathcal{T}}$, instead of a minimum. It also ensures that the shift is a smooth function of T . If p is not correctly chosen the shift can jump discontinuously instead of becoming smoothly displaced outside the first Ramsey fringe. For the experimental regimes described here, no discontinuity occurs and we can set $p = 0$.

An important point to emphasize is the different dependence of the shift on T in the weakly and strongly interacting regimes. In the weakly interacting regime, $TV^{\alpha, \beta} \ll 1$ and $TU^{eg} \ll 1$, the \mathcal{B} term provides the leading contribution, because it exhibits a linear dependence on interactions $\mathcal{B} \propto (TV^{\alpha, \beta}, TU^{eg})$. This results in a T -independent collision shift. On the other hand, in the strongly interacting regime, $(TV^{\alpha, \beta}, TU^{eg}) \gg 1$, both terms \mathcal{B} and \mathcal{A} exhibit a nontrivial sinusoidal dependence on the various interaction parameters. This implies that as T increases, both \mathcal{B} and \mathcal{A} exhibit faster but bounded oscillations and therefore, according to Eq. 13, on average the shift decays as $1/T$.

INTERACTION SIDEBANDS: RABI SPECTROSCOPY

We consider now the case in which the system is interrogated during a long single Rabi pulse of duration t . In this situation, both interaction- and laser-driven terms must be accounted for at the same time during the dynamical evolution. For s -wave-dominated collisions, reaching the strongly interacting regime $U^{\alpha\beta}t > 1$ can lead to a suppression of the clock shift [17, 19, 30]. This is not necessarily the case for p -wave-dominated collisions, in which atoms interact even in the initially populated triplet manifold.

Moreover, if $(V^{eg} - V^{gg})t > 1$ and the atoms start in the triplet $|gg\rangle$ state, there is a large gap that they must overcome if $\delta t \ll 1$ to populate the $\frac{1}{\sqrt{2}}(|ge\rangle + |eg\rangle)$ state. This means that only when $\delta = V^{eg} - V^{gg}$ do the two states become resonant, and population will be transferred between $|gg\rangle$ and $\frac{1}{\sqrt{2}}(|ge\rangle + |eg\rangle)$. Since $|gg\rangle$ is coupled to $|ee\rangle$ by a second-order process, population of $|ee\rangle$ is energetically suppressed. Only if $\delta = \frac{C_{n_1, n_2}^i}{\Omega^2/B_{n_1, n_2}}$ is there a two-photon resonance, but even in this case the overall amplitude is small since it is proportional to $\Omega^2/B_{n_1, n_2}$.

From these considerations, one can write the lineshape of the 2D lattice array as

$$N^e(T, \delta) = \left\langle \sum_{i=1}^{N_1} \rho[\sqrt{2}\bar{\Omega}_{n_1, n_2}^i, \delta - V_{n_1, n_2}^{eg, i} + V_{n_1, n_2}^{gg, i}] + \sum_{i=1}^{N_1} \rho \left[\sqrt{2} \frac{(\bar{\Omega}_{n_1, n_2}^i)^2}{B_{n_1, n_2}^i}, \delta - \frac{C_{n_1, n_2}^i}{2} \right] + \sum_{i=1}^{N_1} \rho[\sqrt{2}\Delta\Omega_{n_1, n_2}^i, \delta - U_{n_1, n_2}^{eg, i} + V_{n_1, n_2}^{gg, i}] + \sum_{i=1}^{N_0} \rho[\Omega_{n_1}^i, \delta] \right\rangle_{\mathcal{T}} \quad (14)$$

with $\rho[x, y] = \frac{x^2}{x^2+y^2} \sin^2[\sqrt{x^2+y^2}t/2]$. For comparison with experiment, we need to average over the tube array and evaluate thermal averages. If it were possible to resolve the various peaks we would expect the line shape to have three single-photon resonances: One at $\delta = 0$ coming from single occupied tubes, one p -wave related at $\delta \propto \langle V^{eg} - V^{gg} \rangle_{\mathcal{T}}$, and one at $\delta \propto \langle U^{eg} - V^{gg} \rangle_{\mathcal{T}}$ due to s -wave collisions.

To obtain the excitation fraction and the interaction sidebands, we need to properly integrate over the spatial degrees of freedom of the lattice. The characteristic harmonic oscillator frequencies ω_i ($i = X, Y, Z$) of each lattice site vary smoothly with the position of the lattice site modifying the Lamb-Dicke and interaction parameters. The variation of the trapping frequencies is obtained from the lattice potential

$$V(X, Y, Z) = -V_{X,0} \cos^2\left(\frac{\pi X}{a}\right) e^{-\frac{2(Y^2+Z^2)}{w^2}} - V_{Y,0} \cos^2\left(\frac{\pi Y}{a}\right) e^{-\frac{2(X^2+Z^2)}{w^2}}, \quad (15)$$

where a is the lattice spacing, $W \sim 35 \mu\text{m}$ is the beam waist, and $V_{X,0}$ and $V_{Y,0}$ are the lattice depths. We extract the characteristic harmonic oscillator frequencies of a given site by expanding the lattice potential at the center of it. Assuming a uniform occupation of the sites in the center of the lattice, we transform the spatial integration into an integration over the relevant range of trapping frequencies weighted by the number of sites with such trapping frequencies. For each set of trapping frequencies, a thermal average is carried out over both the harmonic oscillator modes and lattice vibrational modes.

This procedure is significantly simplified by noting that the main correction of the spatial average comes from the changes in the interaction terms. Thus, changes in the Rabi frequencies are accounted for only by using an average value, allowing us to transform the integration over trapping frequencies into an integration over interaction strengths.

OTHER CONSIDERATIONS

We have restricted so far our analysis to an effective one-dimensional system with at most two atoms per tube. For more than two atoms per tube the spin model is no longer diagonal in the collective spin basis, since the spin Hamiltonian is not $SU(2)$ symmetric. This implies that for more than two atoms and outside the weakly interacting regime our calculations are not exact. However, we have performed numerical calculations for up to five atoms per tube that show that the two-atom model can qualitatively predict the many-atom case, but with renormalized interaction parameters.

In the 1-D lattice there are two weakly confined directions and multiple atoms per lattice site. Under these conditions, interaction-induced mode-changing collisions, which are not accounted for in our two-atom model [17], have to be included. We have studied the role of those processes by numerical evaluation of a more general multi-mode Hamiltonian and found that it mainly leads to a renormalization of the model parameters. All of these considerations justify the validity of the two-atom model for the description of the 1-D lattice.

EXPERIMENTAL DATA ON VARIOUS PULSE DURATIONS

We use short Ramsey pulses ($t_{1,2} \sim 1\text{ms}$) to avoid interaction effects during the pulse. However, for pulses shorter than the mean oscillation period in the trap, $\Omega \gtrsim \omega_i$ with i the weakest trap direction, and laser-induced mode-changing collisions (not included in the two-atom model) are not necessarily suppressed. To explore the role of laser-induced mode-changing collisions, we measured the collision shift as function of excitation fraction in the 2-D lattice for various pulse durations. As shown in Figure 4, we varied the pulse time $t_{1,2}$ by one order of magnitude but found no substantial change in the measured shifts. Thus we conclude that these processes do not play an important role.

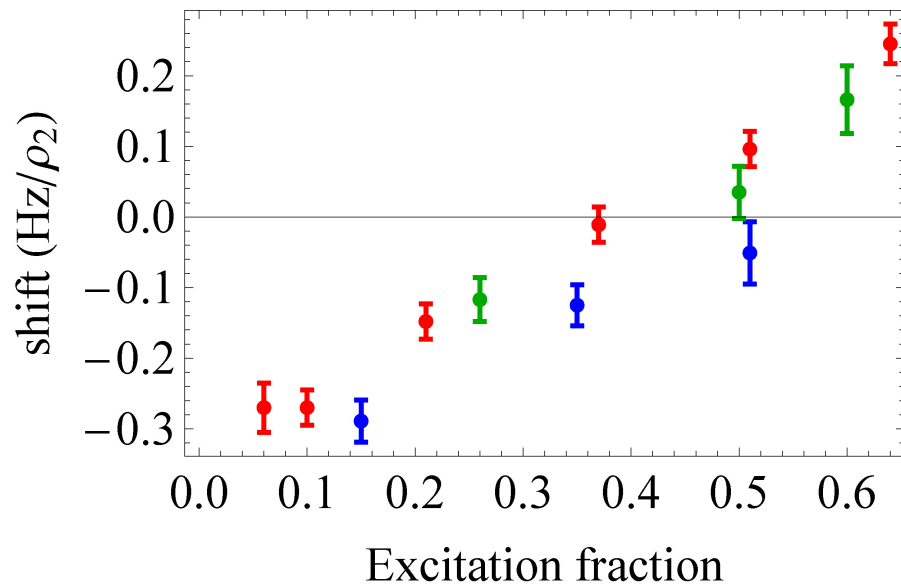


FIG. 4: We study laser-driven mode-changing collisions by measuring the collisional frequency shift vs. excitation fraction for various Ramsey pulse times in the 2-D lattice. The blue, red, and green points correspond to $t_{1,2} = \{0.5, 1, 5\}$ ms, respectively. Because we observe no substantial trend, we conclude that these processes do not play an important role.